

Structure of Biaxially Oriented Polypropylene Film

HIROZO UEJO and SADA O HOSHINO, *Hirakata Plastics Laboratory, Ube Industries Ltd., Hirakata, Osaka, Japan*

Synopsis

Isotactic polypropylene hot-pressed film was subjected to uniaxial and biaxial stretching. The orientation behavior was investigated by means of x-ray pole figure technique, birefringence, electron microscope, and tensile tester. From the x-ray pole figure results it was confirmed that three kinds of crystal orientations, i.e., c-axis along the stretching direction, b-axis normal to the plane of the film, and [110] vector weakly normal to the film, accompany the biaxial stretching of the film. Electron micrographs of the surface of biaxially stretched polypropylene film revealed that, as the elongation increased, fibrillar structures became oriented to the stretching directions. From this orientation behavior a new deformation mechanism based on the woven structure presented by Khoury et al. was proposed. In this mechanism the orientation of the crystals is explained as a phenomenon accompanying the rotation and splitting of the woven structure presumed to be the structural element of polypropylene film.

INTRODUCTION

It has been pointed out by several authors that rolled or biaxially stretched polypropylene film exhibits unique crystal orientation. Sobue and Tabata¹ reported that the (040) crystallographic plane becomes oriented parallel to the plane of rolling. Wilchinsky² determined the degree of c-axis orientation of the rolled polypropylene film by means of the x-ray pole figure technique and concluded that the cold rolling produces a preferred orientation of c-axis in the plane defined by the rolling direction and normal to the film, which was attributed to the local necking of the sample during the deformation.

Okajima et al.^{3,4} studied the crystal orientation behavior of two-step biaxially and polyaxially oriented film by optical and x-ray methods and came to the conclusion that molecular chains are oriented randomly in the plane of the film during polyaxial stretching processes. They also found a preferential orientation of the b-axis perpendicular to the surface of the film as reported by Sobue and Tabata.¹

Recently, Kawai and Takahara⁵ reported the identical conclusion concerning the preferential orientation of b-axis from the result of x-ray pole figure studies on biaxially stretched polypropylene film. In addition to the preferential orientation of the b-axis, complex crystal orientations were also proposed from the analysis of pole figure diagrams, the origin of which are not obvious at present.

In this paper we attempted to carry out a detailed study on the orientation behavior of polypropylene film under biaxially stretching by various means such as the x-ray pole figure method, birefringence measurement, electron microscopy, and mechanical measurements. Comparing the results obtained by these experimental methods, we found it possible to propose a novel deformation mechanism by which the crystal orientation behavior of biaxially oriented polypropylene film can be explained more satisfactorily. The concept of woven structure^{6,7} proposed as the elemental texture of polypropylene crystal aggregates was utilized as the basis for our present proposition.

EXPERIMENTAL

Isotactic polypropylene having $[\eta] = 2.21$ in Decalin at 130°C was used as a raw material for our study. A laboratory-type biaxial stretching apparatus for polymer film manufactured by Iwamoto Seisakusho, Kyoto, Japan, was used for the orientation of the film. With this apparatus it is possible to stretch the sample uniaxially or biaxially and continuously or stepwise by means of a pantograph-type stretching device. Polypropylene film cast from the melt in a hot press was stretched at 145°C up to a given elongation ratio in a hot air circulating thermostatted oven.

X-Ray pole figure diagrams of the stretched samples were obtained by an x-ray diffractometer equipped with a pole figure goniometer designed by Shimadzu Seisakusho Co., Kyoto. Ni-filtered copper radiation was used as the x-ray source. Both transmission and reflection methods developed by Decker et al.⁸ and Field and Marchant,⁹ respectively, were carried out so that we might cover the whole range of crystal orientation. X-Ray data thus obtained were processed by a Facom 270-20 electronic computer for the necessary corrections described elsewhere.¹⁰

Birefringence of the film was measured by the tilting method proposed by Stein.¹¹ Three principal refractive indices of the oriented samples were calculated from the optical data by the combination of the Berek compensator and a universal stage which permits the tilting of the sample with respect to the light passing through the polarized microscope. From the refractive index values we can obtain the orientation parameters that characterize the molecular orientation of the specimen. The procedures for the determination of orientation parameters from birefringence values have been discussed by Kawai et al.,¹² and we followed their procedure.

The two-step replication (Cr-shadowing and carbon evaporation) method was applied to investigate the structure of the sample morphologically by means of an electron microscope. The stress-strain behavior of the biaxially oriented film was studied by using an Instron tensile tester at room temperature at an elongation rate of 400%/min.

RESULTS AND DISCUSSION

In general, the orientation behavior of polymer films depends greatly on the orientation conditions, such as elongation rate, elongation temperature,

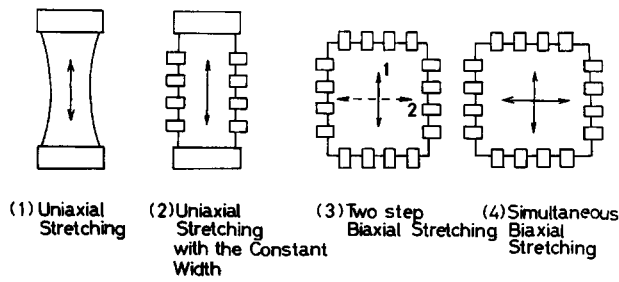


Fig. 1. Schematic diagram of procedures of elongation.

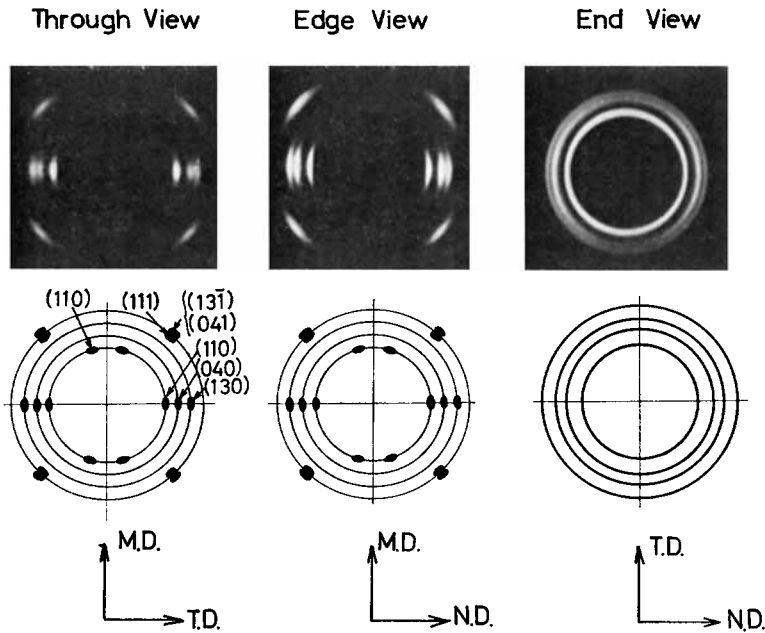


Fig. 2-1. X-Ray diffraction patterns of constant-width uniaxial film (elongation ratio $\times 5$).

or how the sample is stretched, that is, uniaxially or biaxially. In order to compare the orientation behaviors we varied the stretching method as illustrated in Figure 1 and studied the crystal orientation of polypropylene film by various experimental means.

The oriented samples were prepared by four different ways: (1) uniaxial stretching, (2) uniaxial stretching maintaining the width of the sample identical to the original width by clamping the edge of the sample during the stretching, (3) two-step biaxial stretching, and (4) simultaneous biaxial stretching (Fig. 1).

From x-ray and birefringence results shown in Figure 2 it is evident that constant-width uniaxial stretching does not provide us with completely

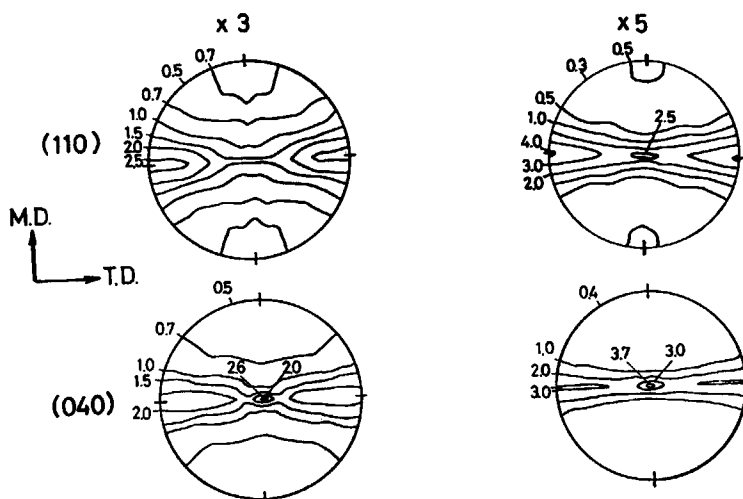


Fig. 2-2. X-Ray pole figure diagrams of constant-width uniaxial film (elongation ratios $\times 3$ and $\times 5$). Vectors $[110]$ and $[040]$.

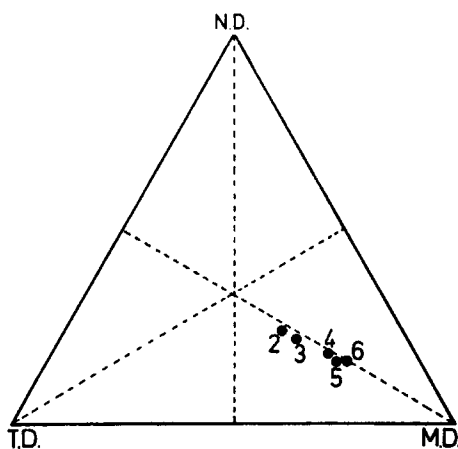


Fig. 2-3. Orientation triangular diagram of constant-width uniaxial film.

cylindrical symmetry around the stretching direction (denoted as M.D., or machine direction, hereafter; T.D. denotes transverse direction; and N.D., the direction normal to the film) as encountered in the case of simple uniaxial stretching. As seen from the pole figure diagrams in Figure 2, both $[110]$ and $[040]$ vectors exhibit preferred orientation in the plane normal to the machine direction (end view); $[110]$ vectors show slightly stronger preference for the direction parallel to the film ($\alpha = 0^\circ$), and $[040]$ vectors show a more pronounced preference for the direction normal to the film ($\alpha = 90^\circ$). A weak orientation of $[110]$ vectors in the machine direction as seen in the through- and edge views is attributed to a a^* -axis orientation¹³ similar to that reported for stretched isotactic polypropylene monofilament.

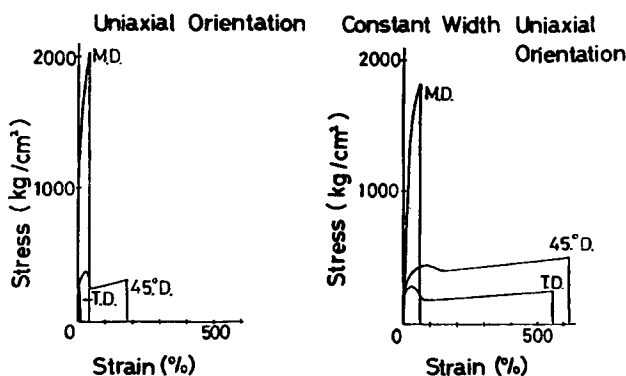


Fig. 3. Stress-strain behavior of uniaxial and constant-width uniaxial film in three directions: M.D. = machine direction; 45°D. = 45° diagonal; T.D. = transverse direction.

Figure 3 shows the stress-strain behavior of uniaxial and constant-width uniaxial film. As expected from the crystal orientation behavior described above, the latter shows higher elongation along the transverse and diagonal directions than the former.

When the sample is stretched stepwise in directions at right angles, the crystals become oriented preferentially with respect to both stretching directions, as shown in the pole figure diagrams in Figure 4. The orientation of $[110]$ vectors is influenced greatly owing to the increase of the second elongation. The diffraction intensity of $[110]$ is maximized at the positions where $\alpha = 20^\circ$, $\beta = 0^\circ$ and 90° , and $\alpha = 0^\circ$, indicative of the preferential orientation of $[110]$ vectors to the M.D.(1) and M.D.(2). With regard to the samples stretched stepwise along two directions to equal extent, symmetrical pole figure patterns as illustrated in Figure 4 are obtained. Concerning $[040]$, the greater the elongation ratio, the higher the intensity at $\alpha = 90^\circ$, namely normal to the film surface. In the case of 5×5 - and 5×7 -stretched film, however, a small amount of diffraction intensity is observed at the position $\alpha = 20^\circ$ and $\beta = 90^\circ$, as shown in Figure 4. This indicates that the biaxial orientation is governed by complex crystal orientation mechanisms.

The triangular orientation diagram of the stepwise biaxial film obtained from birefringence measurement is shown in Figure 5. Owing to the second stretching, the molecular chains tend to get aligned normal to the surface of the film at the initial stage of elongation. Passing beyond the balance point (3×3 and 5×5), they become oriented in the direction of the second stretching lying in the plane of the film. Figure 6 shows the electron micrographs of the surface of the two-step biaxially oriented film. In the left micrograph (5×3), one can observe the small fibrillar structures tilted slightly to the second stretching direction. In the right one (5×5), small lattice-like structures are observed to be oriented to M.D.(1) and M.D.(2). It seems that preferential orientation of fibrillar structures along the two stretching directions is consistent with the x-ray pole figure dia-

grams shown in Figure 4. From the standpoint of mechanical properties, these samples are anisotropic according to the directions of stretching as illustrated in Figure 7.

Finally, in the case of simultaneous biaxial orientation, we obtained samples in which the molecular chains are oriented randomly in the plane of the film typical of biaxially oriented polymer films. The x-ray patterns

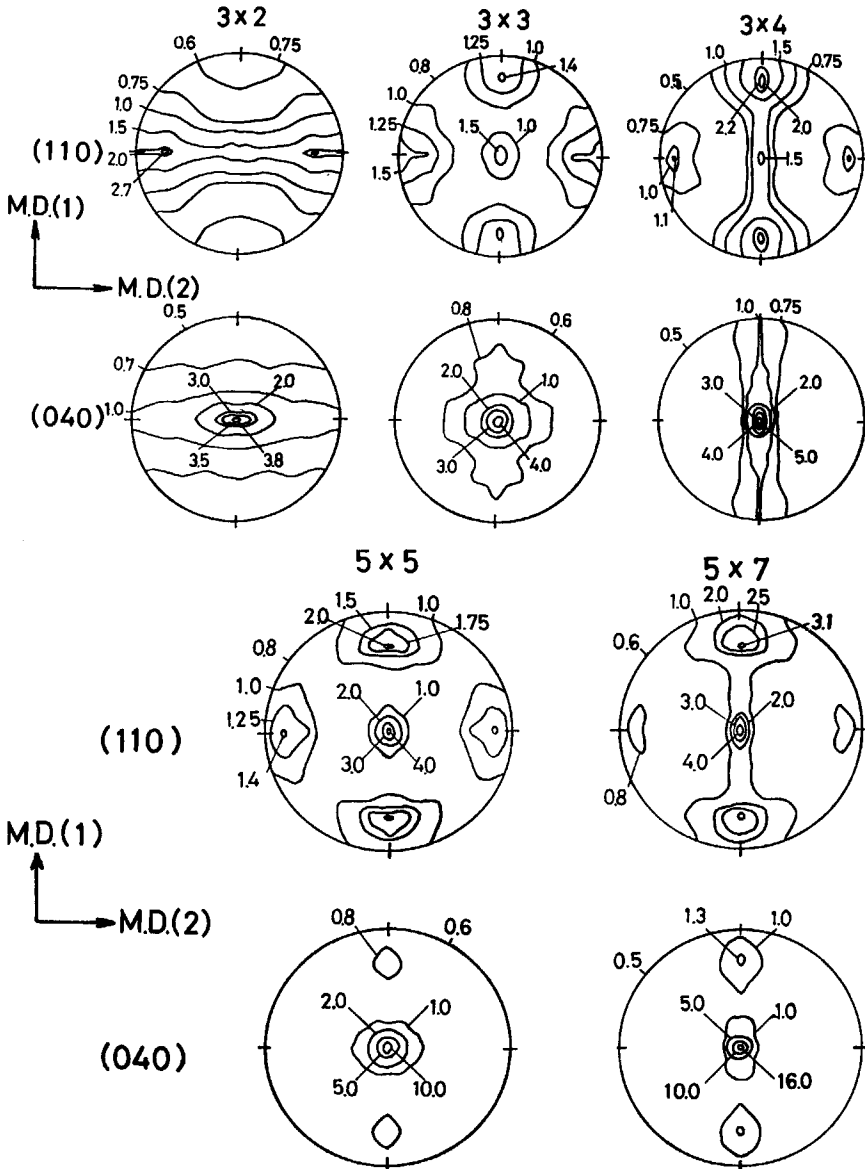


Fig. 4. X-Ray pole figure diagrams of two-step biaxial film (elongation ratios 3×2 , 3×3 , 3×4 , 5×5 , and 5×7). Vectors [110] and [040].

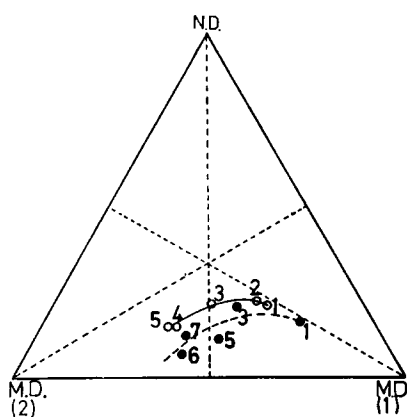


Fig. 5. Orientation triangular diagram of two-step biaxial film: (O) first stretching, $\times 3$; (●) first stretching, $\times 5$.

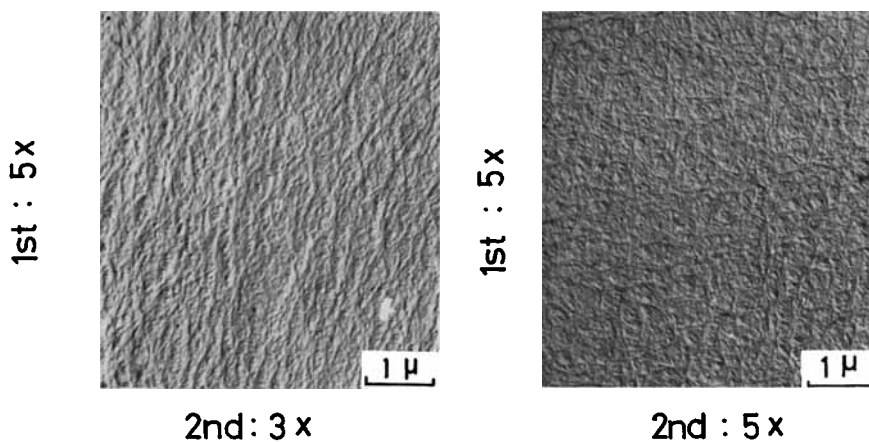


Fig. 6. Electron micrographs (surface replica) of two-step biaxial film (elongation ratios 5×3 and 5×5).

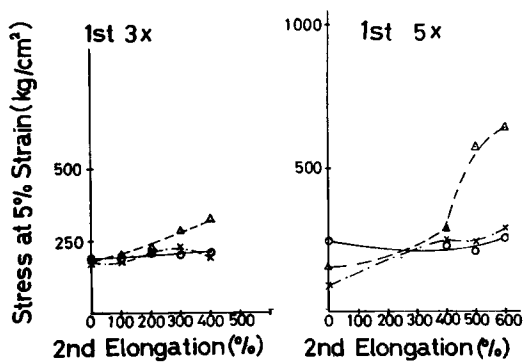


Fig. 7. Stress at 5% strain vs. the second elongation ratio with regard to two-step biaxial film: (O) M.D.; (Δ) T.D.; (X) 45° D.

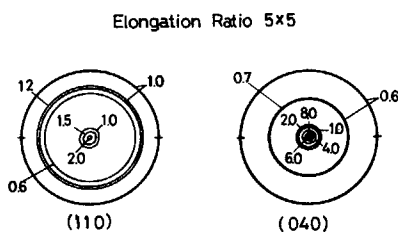


Fig. 8. X-Ray pole figure diagrams of simultaneous biaxial film (elongation ratio 5×5). Vectors $[110]$ and $[040]$.

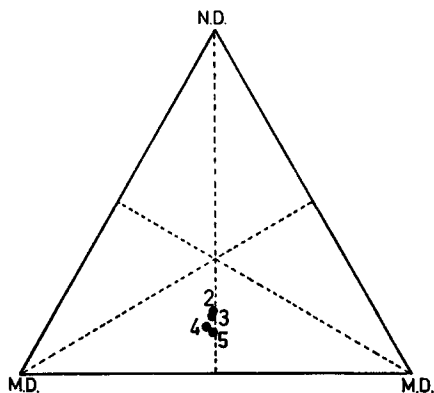


Fig. 9. Orientation triangular diagram of simultaneous biaxial film.

from the edge or end direction show that the b -axis is oriented perpendicularly to the surface of the film, agreeing with the results obtained by other investigators.¹⁻⁵

In addition to the preferential orientation of the b -axis, the $[110]$ vectors had an orientation distribution with the strongest maximum aligned normal to the surface of the film, while a smaller maximum occurred at $\alpha = 20^\circ$, as the pole figure diagrams indicate in Figure 8. The higher the elongation, the more the $[110]$ vectors become oriented at about 20° with respect to the plane of the film. From the birefringence measurement the refractive index values decrease along the normal to the film and the molecular chains become oriented parallel to the plane of the film, as shown in Figure 9.

In the electron micrograph of simultaneously drawn biaxial film, one can observe randomly oriented fine fibrils, as shown in Figure 10, supporting the x-ray pole figure results shown Figure 8. The mechanical properties of this type of film are balanced in various directions, as shown in Figure 11, indicating the isotropic nature of the samples.

Crystal Orientation Mechanism

In order to describe the crystal orientation behavior observed with the various types of stretched polypropylene film as described above, four kinds of crystal orientations—A(1), A(2), B, and C, as illustrated in Figure

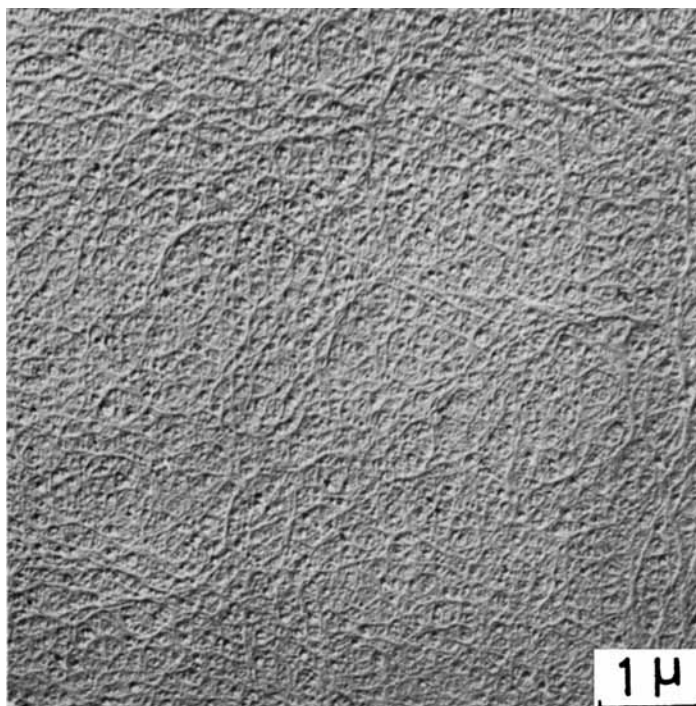


Fig. 10. Electron micrograph (surface replica) of simultaneous biaxial film (elongation ratio 5×5).

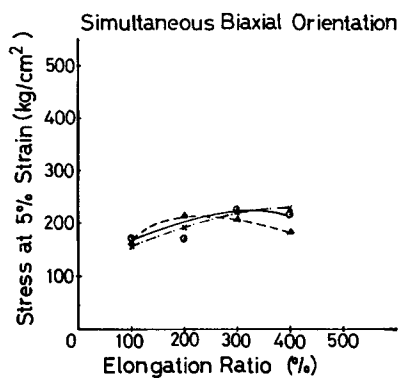


Fig. 11. Stress at 5% strain vs. the second elongation ratio with regard to simultaneous biaxial film: (O) M.D.; (Δ) T.D.; (\times) 45° D.

12—were proposed to be the main types of crystal orientation. We assume that intermediate states of orientation can be represented as some combination of these basic types. A(1)- and A(2)-type orientations have the c-axis oriented along the two machine directions at right angles, to each other. On the other hand, B- and C-type orientations are those of b-axis and [110] vectors normal to the plane of the film, respectively.

While the simple uniaxial orientation of the sample causes A(1)-type and a small amount of a*-axis orientations, in the case of constant-width uniaxial orientation, A(1)- and B-type orientations are prevalent at the

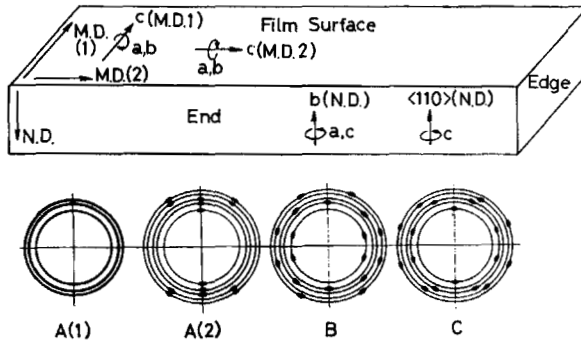


Fig. 12. Schematic diagram of the four kinds of crystal orientation and x-ray diffraction patterns expected from them.

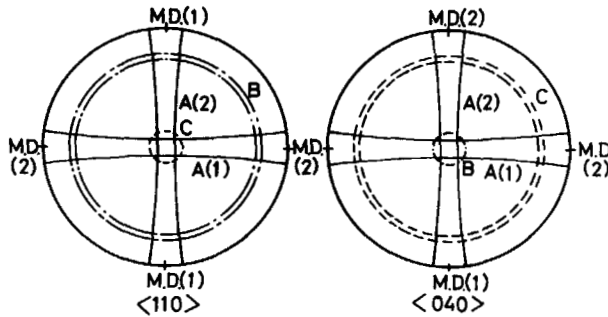
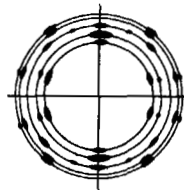
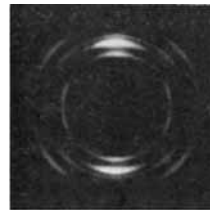


Fig. 13. X-Ray pole figure diagrams expected from the overlap of A(1)-, A(2)-, B-, and C-type crystal orientations concerning two-step biaxial film. Vectors [110] and [040].

X-Ray Diffraction Pattern
Obtained by the Overlap
of Proposed Orientation



Simultaneous
Biaxial Orientation



Edge(End) View



Fig. 14. X-Ray diffraction patterns of simultaneous biaxial film, experimentally obtained and expected theoretically.

same time. In the case of two-step biaxial orientation, the main contributions are ascribed to A(1)- and A(2)-type orientations. When, however, additional contributions from B- and C-type orientations are taken into account, the diffraction intensity is considered to be maximized in the regions around $\alpha = 17^\circ$ and $\beta = 0^\circ$ and 90° where the overlap of diffraction intensities of A(1)-, A(2)-, and B-type orientations takes place as shown in Figure 13. This result agrees very well with the pole figure diagrams shown in Figure 4.

With regard to the simultaneous biaxial orientation, the x-ray pattern given in Figure 14 is well explained by assuming a mixture of random orientation and B- and C-type orientations. Consequently, it is concluded that the crystal orientations characteristic of biaxially oriented polypropylene films may be resolved into the combination of c-axis preferential in the plane of the film and b-axis and [110] vectors normal to the plane of the film.

Deformation of the Superstructure of Polypropylene Film During Stretching

From the x-ray diffraction studies, it has become evident that a combination of three types of crystal orientation may be assumed for the biaxially oriented polypropylene film. We attempted to interpret the origin of these crystal orientations by proposing a new deformation model. If we assume that polypropylene hot-pressed film is composed mostly of the

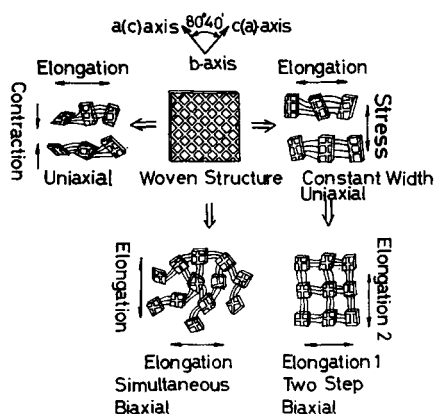


Fig. 15. Deformation mechanism of the superstructure of polypropylene film based on "woven structure."

woven structures proposed by Khoury⁶ and Padden and Keith⁷ during the stretching at higher temperatures, then the structural elements of such woven structure would not deform greatly owing to the high elongation temperature. Within the woven structure, one should note that the crystal *b*-axis is aligned normal to the plane of the film, as shown in Figure 15

(Kubo and Kobayashi¹⁴ claim that the b-axis is tilted 9° to the normal to the film).

At first in the case of uniaxial orientation, the structural elements of woven structure are oriented randomly around the elongation axis, which corresponds to the A(1)-type orientation described in the previous section. Biaxial orientation causes the woven structure to become aligned parallel to the plane of the film and the crystal b-axis to be oriented perpendicularly to the plane of the film. When the film is stretched uniaxially while keeping the width constant, a similar type of orientation takes place. Hence we can find some of the b-axis to be oriented normal to the film surface in such constant-width stretching. The difference between the stepwise and simultaneous biaxial orientation lies in that in the former the fibrillar structure is oriented comparatively parallel to the elongation direction, whereas in the latter it is oriented randomly as shown in Figure 15.

Thus we believe that we can explain the possibility of b-axis orientation accompanying the biaxial orientation by this deformation model. At the higher elongation, however, [110] vectors orient perpendicularly to the surface of the film as well. In addition, the higher the elongation ratio, the more will the woven structure be destroyed. Finally the fiber structure will appear. The structure corresponding to this fiber-type crystal orientation is not yet clear.

The authors wish to thank Professor K. Kobayashi and Dr. T. Nagasawa for their kind discussion with us and Mr. T. Yoshikawa for his experimental work.

References

1. H. Sobue and Y. Tabata, *J. Appl. Polym. Sci.*, **2**, 62 (1959).
2. Z. W. Wilchinsky, *J. Appl. Polym. Sci.*, **7**, 923 (1963).
3. S. Okajima, K. Kurihara, and K. Homma, *J. Appl. Polym. Sci.*, **11**, 1703 (1967).
4. S. Okajima and K. Homma, *J. Appl. Polym. Sci.*, **12**, 411 (1968).
5. H. Kawai and H. Takahara, Paper presented at First Kansai Seminar on Fibers, Osaka, Japan, March 1968.
6. F. Khoury, *J. Res. Natl. Bur. Std.*, **70A**, 383 (1966).
7. F. J. Padden, Jr., and H. D. Keith, *J. Appl. Phys.*, **37**, 4013 (1966).
8. B. F. Decker, E. T. Asp, and D. Harker, *J. Appl. Phys.*, **19**, 388 (1948).
9. M. Field and M. E. Marchant, *J. Appl. Phys.*, **20**, 741 (1949).
10. R. S. Stein, J. Powers, and S. Hoshino, *ONR Technical Report No. 33*, University of Massachusetts, Amherst, July 7, 1961.
11. R. S. Stein, *J. Polym. Sci.*, **24**, 383 (1957).
12. H. Kawai, H. Takahara, Y. Yamaguchi, and A. Fukushima, *Sen-i Gakkaishi*, **25**, 60 (1969).
13. H. Awaya, *J. Chem. Soc. Japan, Pure Chem. Sec.*, **82**, 1575 (1961).
14. S. Kubo and K. Kobayashi, Japan Chemical Society Meeting, May 1968.

Received September 26, 1969